

LOCAL SCOUR AND RIPRAP PROTECTION DOWNSTREAM WATER SPILLWAYS

Rabiea I. Nasr and Hossam M. Nagy

Irrigation and Hydraulics Department, Faculty of Engineering,
Alexandria University, Alexandria-21544, Egypt.

ABSTRACT

A theoretical approach has been derived to describe local scour downstream the floor of hydraulic structures, such as weirs, spillways, and regulators. Based on the fundamentals of fluid mechanics, an expression for relative maximum scour depth is analytically presented with the exception of a single experimental parameter. Experimental work is conducted on two different laboratory flumes for simulating scour process downstream weir construction. Series of runs are performed on weirs with different floor lengths, describing local scour geometry, depth and length, and flow pattern in terms of velocity measurements at different sections in that region. Only one parameter in the theoretical expression is estimated by using the measured experimental data. Time effect on the development of scour hole geometry has been investigated, and presented in predictive expressions. Characteristics of scour geometry and bed protection works, riprap, are experimentally studied through additional group of runs by using natural uniform riprap instead of increasing floor length. The advantage of this study is that, it has theoretical base more than other previous studies which provide empirical expressions of dimensional analysis.

Keywords: Weir structure, Local scour, Particles stability, Shear stress, Riprap.

INTRODUCTION

Local scour downstream water structure is one of the dangerous problems which are facing irrigation engineers. Design procedures of such constructions should include protective measures against scour in order to prevent damage or complete failure of the structure. Because of this, a comprehensive investigation should be done on the scour causes, mechanism, scour hole geometry, flow structure, and scour development with passage of time. Several previous studies of local scour downstream hydraulic structures were presented [1-6]. Most of the presented studies are based mainly on dimensional analysis and empirical formulae.

The present paper concerns the process of local scour downstream hydraulic jump, through a theoretical approach calibrated with the measured experimental data. The approach depends mainly on one dimensional continuity equation and

momentum equation with the assistance of velocity distribution relations which were investigated by Schlichting [7] and then developed for application by Tsubaki and Hirano [8]. In the experiments, the flow passed over weir crest making hydraulic jump, then passed over sudden change in bed roughness from a fixed floor surface to a movable bed of sand under the dynamic condition. Measurements of scour hole were taken in equilibrium state and also during the development process. An expression for relative maximum scour depth was obtained. A relation between maximum scour depth and length was demonstrated. The progress of scour process with passage of time was described graphically and then represented analytically. A qualitative description of the advantages of replacing a specific length of the floor with riprap material is presented.

FLOW PATTERN DOWNSTREAM WEIR STRUCTURE

Considering steady, uniform, two dimensional flow downstream a hydraulic jump which occurs over the downstream floor of a weir structure. The flow pattern over the non-cohesive stream bed just after the floor edge is well described as shown in Figure 1. In the developed scour hole, turbulent motion of the fluid is assumed, and bottom velocity along the surface of scour hole has two directions; upward face has bottom velocity toward downstream, while downward face has velocity toward upstream. The lowest point, re-attachment point C, is assumed to have a bottom velocity which causes critical shear stress, and the particles are under equilibrium state.

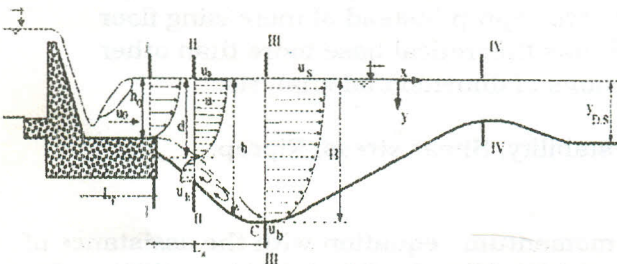


Figure 1 Schematic sketch of flow pattern in local scour hole

From geometrical properties of velocity distribution curve in sec II-II,

$$\frac{u}{u_s} = f(\zeta_1), \zeta_1 = 1 - \frac{y}{d} \text{ for } (0 \leq y < d) \quad (1)$$

$$\frac{u}{u_s} = f_2(\zeta_2, \eta), \zeta_2 = \frac{y-d}{h-d}, \eta = \frac{x}{h_0} \text{ for } (d \leq y \leq h) \quad (2)$$

For section III-III,

$$u = u_b + u_s f(\zeta_1, \eta), \zeta_1 = 1 - \frac{y}{H} \quad (3)$$

where u is the local flow velocity at any point, u_s is the surface velocity, u_b is the bottom velocity, y is the vertical scale measured from the water surface, x is the horizontal scale, d is the depth from the surface to zero velocity, h is the total flow depth, h_0 is the water depth over the edge of the floor, and H is the water depth over the lowest point of the scour hole.

Applying continuity equation between sec. I-I and sec. III-III,

$$u_0 h_0 \int_0^H u_b dy + \int_0^H u_s f(\zeta_1) dy \quad (4)$$

where u_0 is the average velocity at sec. I-I. From the above equations,

$$u_0 h_0 = H (u_b - u_s G_1) \quad (5)$$

where $G_1 = \int_1^0 f(\zeta_1) d\zeta_1$. Considering the control volume (abcde), and applying momentum equation between sections I and III,

$$\rho \beta u_0^2 h_0 - \rho \int_0^H u^2 dy = \frac{1}{2} \rho g H^2 - \frac{1}{2} \rho g h_0^2 \quad (6)$$

where ρ is flow density, β is momentum correction factor, and g is gravitational acceleration.

$$\int_0^H u^2 dy = \int_0^H [u_b + u_s f(\zeta_1)]^2 dy \quad (7)$$

$$= H(u_b^2 - 2u_b G_1 - u_s^2 G_2) \quad (8)$$

where $G_2 = \int_1^0 f^2(\zeta_1) d\zeta_1$, From

$$\text{Equation 5, } u_s = \frac{1}{G_1} (u_b - u_0 \frac{h_0}{H})$$

Substituting into Equation 8.

$$\int_0^H u^2 dy = -H [(G_3 + 1) u_b^2 - 2(G_3 + 1) u_0 u_b \frac{h_0}{H} + G_3 u_0^2 (\frac{h_0}{H})^2] \quad (9)$$

where $G_3 = G_2 / G_1^2$, Substituting into Equation 6.

$$\frac{H}{h_0} = \sqrt{1 + 2F_0^2 [\beta + (G_3 + 1) (\frac{u_b}{u_0})^2 \frac{H}{h_0} - 2(G_3 + 1) \frac{u_b}{u_0} + G_3 \frac{h_0}{H}]} \quad (10)$$

where $F_0^2 = u_0^2 / gh_0$ is the squared Froude number at sec. I-I.

STABILITY OF SEDIMENT PARTICLES

The developed scour hole depth can be estimated by using Equation 10. However, the flow velocity near bed level u_b is difficult to be obtained or measured. The value of

bottom velocity u_b depends mainly on size of sand particles, the location in the scour hole, and the water depth. At the re-attachment point c , stability analysis for sand particles may be presented, assuming equilibrium condition between the particle weight and the hydrodynamic force generated by diffused jet velocity. Since shear stress depends mainly on flow depth, and point c has the maximum depth, therefore, shear stress at such point is assumed to be critical.

$$\tau_{cr} = \psi_c \cdot \rho \cdot s_g D_{50} \quad (11)$$

where τ_{cr} is the critical shear stress, ψ_c is the shields number which is approximately constant at 0.047, s is the specific weight of sediment in water, and D_{50} is the mean particle size.

In general, the bed shear stress can be written in the following form,

$$\tau_b = C_f \rho u_b^2 \quad (12)$$

where C_f is the local friction coefficient which can be presented as a simple function of the relative roughness, see Reference 4.

$$C_f = \frac{\psi_c}{B} \left(\frac{D_{50}}{y_b} \right)^x \quad (13)$$

where B and x are coefficients have the values 2.9 and 0.19, respectively, Bormann [4], and y_b is equal to H at location of maximum scour. Thus, u_b can be presented as follows,

$$u_b = 68.5 \sqrt{D_{50}} \left(\frac{H}{D_{50}} \right)^{0.095} \quad (14)$$

Substituting into Equation 10,

$$\frac{H}{h_0} = \sqrt{1 + 2F_0^2 [\beta + 4.78(G_3 + 1)\chi^2 \left(\frac{H}{h_2} \right)^{11.9} - 4.37(G_3 + 1)\chi \left(\frac{H}{h_0} \right)^{0.095} + G_3 \frac{h_0}{H}]} \quad (15)$$

where $\chi = \frac{1}{F_0} \left(\frac{D_{50}}{h_0} \right)^{0.405}$

EXPERIMENTAL SETUP

The experiments were carried out on two different flumes. The first is a tilting flume of width 86 cm, depth 50 cm, and length 12.0 m with steel bottom and glass wall. A model of sharp edged wooden weir with dimensions 86 cm width and 60 cm height is been installed in the upstream part of the flume. The inclination of weir

downstream face is 1H : 2V. A thin plate weir was placed at the downstream end of the flume to control tailwater depth. The sand which is used in the downstream of the weir structure has mean diameter $D_{50} = 0.948$ mm and standard deviation $\sigma_g = 2.06$. Several runs were conducted to show three dimensional local scour downstream weir construction. The second flume is a steel painted channel with rectangular cross-section of 52 cm in width, total length 13.0 m, and 60 cm in depth. In the upstream reach of the flume, the two sides were made of prospect. A model of sharp edged weir with dimensions 52 cm width, 60 cm height has been installed in the upstream reach. The inclination of the weir downstream face is 1H : 2V. A flap gate was installed in the end of the flume to control down stream water level. Five groups of 23 run were performed. In the first three groups, the movable bed was simulated by graded sand of mean particle size $D_{50} = 0.842$ mm, and standard deviation $\sigma_g = 1.8$. The other two groups were carried out with riprap protection blanket placed after downstream floor of the weir in which the top surface at bed level. The riprap material consists of angular granite crushed stones of uniform size equal to 1.5 inch. The thickness of riprap protection was 15 cm, and riprap lengths were 30 and 60 cm. Figure 2 shows a schematic diagram of the second flume setup, and Figure 3 shows the grain size distribution for bed material in the two flumes.

In both flumes, various discharges were passed to study the effects of flow and sediment parameters on the formation of scour hole. The procedure in each experiment that the down stream was first filled with water to a certain limit, then the run started with low rate of flow, which gradually increased to the specified discharge.

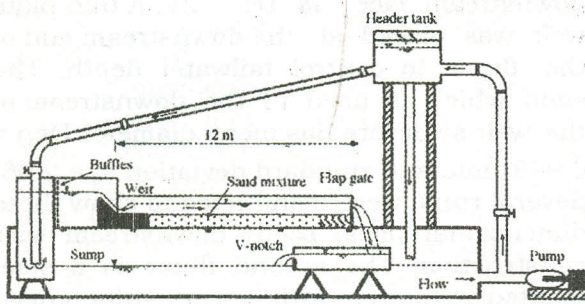


Figure 2 Schematic sketch of the experimental set-up

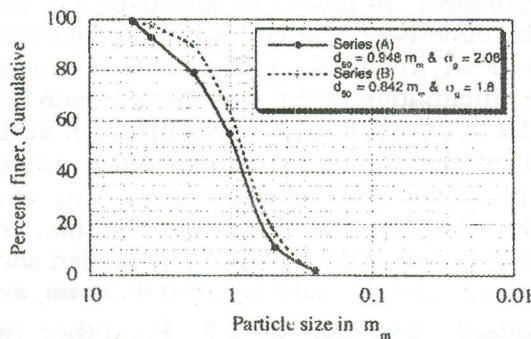


Figure 3. Grain size distribution for bed material

The formed hydraulic jump position was kept over the floor length by controlling the downstream water level. In both flumes, the discharges were measured using two methods; the piezometric tube in the upstream of the triangular weir in the collecting tank, and the point gage which was fixed over the upstream weir structure. The water level was measured by using a point gage with accuracy 0.1 mm, mounted on a mechanical carriage.

The vertical velocity profile for different sections normal to the flow in the tested region was measured by using 2 mm diameter pitot-static tube connected to a sensitive differential piezometers. After getting a fully developed scour hole, 6 hours from the beginning, the test was stopped and water was carefully allowed to drainage through the flume bottom hole covered with woven cloth to prevent the passage of sand through the hole. The levels of developed scour hole downstream the floor or downstream the riprap were measured with the point gage described above. Tables 1. and 2 show summary of experiments and range of parameters under investigation.

Table 1 Summary of Experimental Data (using natural sand for bed)

Run No.	B_w cm	L_w cm	Q lit/sec	y D.S cm	D_{50} cm	sg	F_0	H/ h_0	L_s/h_0
A-1	86	60	32.835	14.3	0.0948	2.06	0.2254	1.62	2.797
A-2	86	60	26.353	12.0	0.0948	2.06	0.2087	1.538	1.538
A-3	86	60	20.748	11.9	0.0948	2.06	0.1876	1.467	1.261
A-4	86	60	13.559	10.7	0.0948	2.06	0.1438	1.368	0.467
A-5	86	60	10.672	10.0	0.0948	2.06	0.1253	-----	-----
B-1-1	52	120	26.206	15.42	0.0842	1.8	0.2657	1.706	2.918
B-1-2	52	120	21.388	14.1	0.0842	1.8	0.2248	1.567	1.418
B-1-3	52	120	16.411	12.73	0.0842	1.8	0.222	1.482	1.178
B-1-4	52	120	6.8702	9.86	0.0842	1.8	0.136	1.4	1.014
B-1-5	52	120	4.92	9.03	0.0842	1.8	0.111	-----	-----
B-2-1	52	90	25.572	15.42	0.0842	1.8	0.265	1.665	2.961
B-2-2	52	90	15.933	12.58	0.0842	1.8	0.219	1.499	1.192
B-2-3	52	90	7.3	10.05	0.0842	1.8	0.141	1.453	1.493
B-2-4	52	90	3.16	8.1	0.0842	1.8	0.084	1.05	0.617
B-3-1	52	60	25.89	15.3	0.0842	1.8	0.2656	1.732	2.941
B-3-2	52	60	15	12.35	0.0842	1.8	0.212	1.487	1.619
B-3-3	52	60	5.78	9.37	0.0842	1.8	0.124	1.395	1.6
B-3-4	52	60	3.07	8.06	0.0842	1.8	0.0825	1.298	1.241
B-3-5	52	60	1.98	7.56	0.0842	1.8	0.058	-----	-----

Local Scour and Riprap Protection Downstream Water Spillways

Table 2 Summary of Experimental Data (using natural sand for bed)

Run No.	B _w cm	L _w cm	L _r cm	Q lit/sec	y D.S cm	L _r cm
R-1-1	52	60	60	26.047	15.38	3.81
R-1-2	52	60	60	16.171	12.65	3.81
R-1-3	52	60	60	60728	9.8	3.81
R-2-1	52	60	30	16.9	12.76	3.81
R-2-2	52	60	30	15.7	12.46	3.81
R-2-3	52	60	30	15.463	12.15	3.81
R-2-4	52	60	30	11.411	11.36	3.81
R-2-5	52	60	30	6.87	9.86	3.81

Calibration of the Model

The parameter which has to be calibrated is the G_3 coefficient of Equation 15. For that purpose, measured values of H/h_0 , F_0 , and D_{50} in the two experimental flumes are used. Momentum coefficient β is assumed to be equal 1.02. Based on fitting of measured and computed results, the G_3 coefficient was found to be dependent on Froude number F_0 , as follows :

$$G_3 = 575 F_0^{2.33} \quad (16)$$

Figure 4 shows the relation between G_3 and F_0 for the experimental data. The fitting curve represents Equation 16 with correlation coefficient $R = 0.983$.

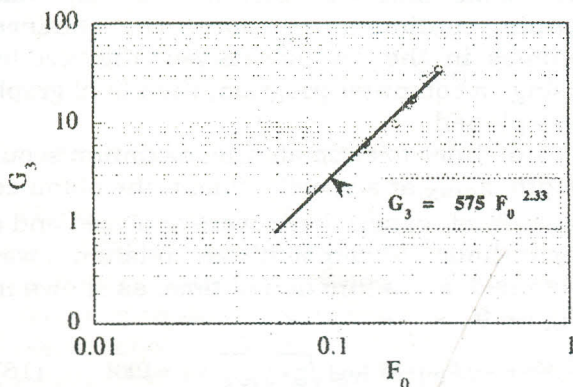


Figure 4 Relation between the coefficient G_3 and F_0

CHARACTERISTICS OF SCOUR DOWNSTREAM THE FLOOR

Geometry of Scour Hole

Figure 5 shows the overview of bed profile in two experiment after 6 hours of

beginning. The scour profile downstream the floor shows a uniform degradation in transverse direction below the section of roughness change, though the scour developed in the vicinity of side walls while an aggradation in bed was recognized in the central part in the downstream. The large scour hole was formed in the central part of the channel and attains the maximum scour depth. The bed level along the side walls became higher than central part because of the interaction of shock waves over the downstream sand bed propagating from the side walls towards the central part of the channel. Figure 6 shows the variation of relative scour length with relative scour depth. The fitting curve gives the following relation :

$$\frac{L_s}{h_0} = 0.33 \left(\frac{H}{h_0} \right)^4 \quad (17)$$

Development Of Scour Profile with Increasing Discharge

Figure 7 compares the final bed profiles of equilibrium states of runs from A-1 to A-5 for different discharges. With the expectation, increasing discharge is creating larger scour depth with the occurrence of accumulation downstream of scour holes. All runs showed similarity in scour hole profile. Also, all runs showed a degradation in bed level at the point of changed roughness, amounting 30% to 50% of maximum scour depth. This is because the fine sand is picked up by local eddies in the

descending face of the holes. For low discharges with Froude number $F_0 < 0.15$, bed undulations, such as two dimensional ripples, were noticed downstream of the scour hole for long distance.

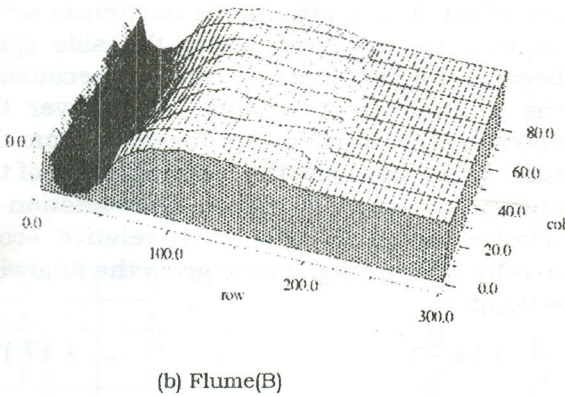
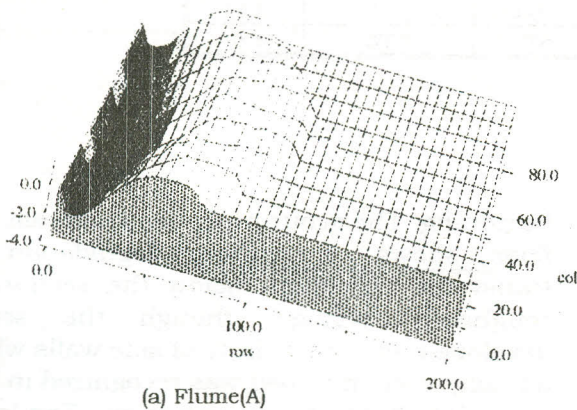


Figure 5 Scour hole configuration in the testing flumes

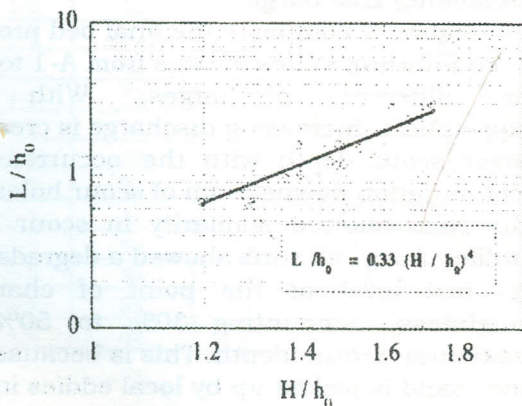


Figure 6 Relation between L/h_0 and H/h_0

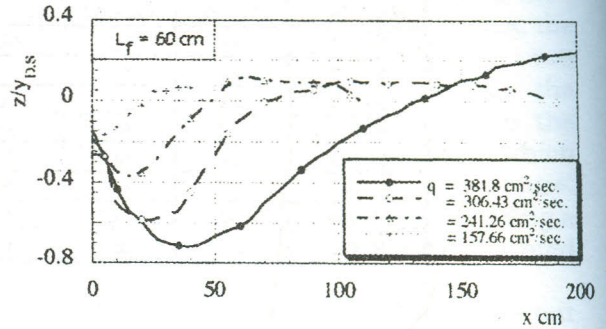


Figure 7 Effect of increasing discharge on scour profile

Development of Scour Profile with Time

To obtain qualitative description about the progress of local scour with passage of time, thin transparency sheets were fixed on the two side walls of the observation reach in the flume. The most appropriate run tests with symmetrical two dimensional scour hole were selected from the total pre-performed run sets. The run with obvious side wall effects is abandoned. Figure 8 shows one of the performed tests. The measured discharge was 16 lit/sec, flume width was 52 cm and normal water depth was 12.6 cm. A stop watch was functioning, and two persons were tracing scour profile on the two sides by using colored markers in the same time for different time intervals within continuous 24 hour. The obtained profiles in the two sheets were digitized by using a computer program, then final graph was plotted.

In order to estimate the maximum scour depth z_{max} at a specific time t , the obtained data from experiments were analyzed and a logarithmic dimensionless relation was obtained as a function of time, as shown in Figure 9.

$$\frac{z_{max}}{y_{D,S}} = -0.5 + 0.25 \log[\sqrt{g/y_{D,S}} \cdot y \cdot t + 100] \quad (18)$$

A similar relation was obtained to predict the relative scour length L_S as a function of time, as shown in Figure 10.

$$\frac{L_S}{y_{D,S}} = -2.2 + 0.85 \log[\sqrt{g/y_{D,S}} \cdot t + 390] \quad (19)$$

Local Scour and Riprap Protection Downstream Water Spillways

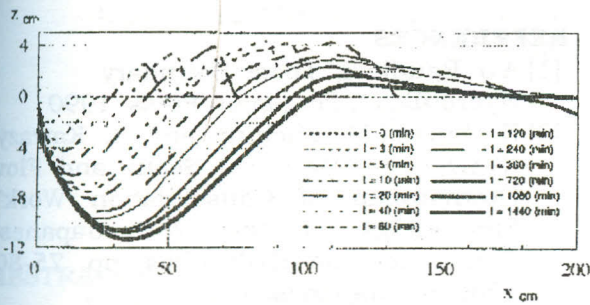


Figure 8 Variation of bed profile with time

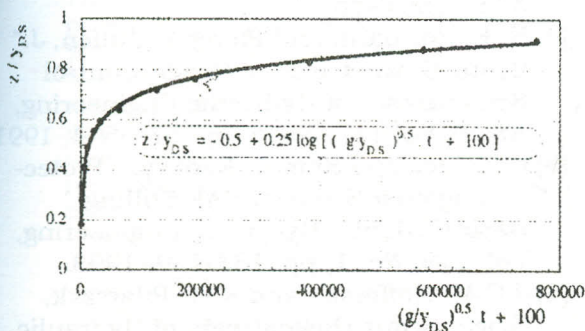


Figure 9 Variation of maximum scour depth with time

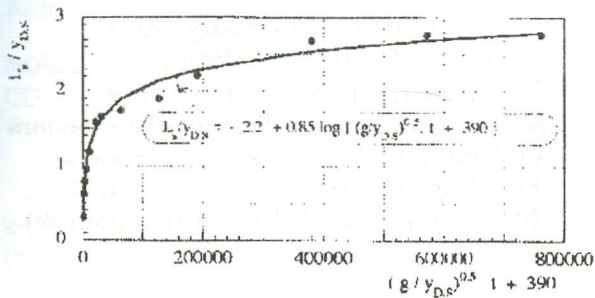


Figure 10 Variation in scour length with time

Riprap Protection Work

Increasing floor length L_f is one of the methods used to prevent scour or to decrease scour process downstream weir construction. This solution can be substituted by using one single thick layer of riprap instead of increasing the construction length. In the experiments, a single layer of riprap with uniform grain size, 1.5 inch, is installed downstream the floor with different lengths in each run. The results of the experiments can be comparatively described well in Figure 11.

The results showed that riprap with length $L_r = 60$ cm is much better than increasing floor with the same length. The ratio between the maximum scour depth in both cases is 0.60, while the ratio of the maximum scour length in case of using riprap is 0.3 the maximum scour length in case of increasing floor length. The design criteria of such riprap should be extensively investigated in further research.

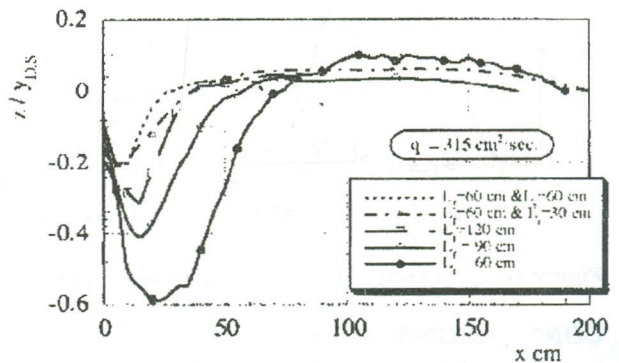


Figure 11 Effect of using riprap on scour profile

Velocity Profile in the Scour Hole and over Riprap

Figure 12 gives the record of velocity distribution in three different vertical sections in the flow pattern over scour hole. It is noticed that the velocity is diminished gradually till the lowest point of the scour hole, then it is increased again with the rise of bed surface. The backward flow over the downward face of the scour hole was not clearly noticed in all measurements, except in two runs of big discharges in the wide flume. In the figure, y_1 represents water depth measured from the bottom. Figure 13 shows the velocity distribution over the uniform riprap in three different vertical sections. It is clear that the distribution is following the logarithmic trend in all cases, and the curvature of velocity profile d^2u/dy_1^2 is positive in all sections.

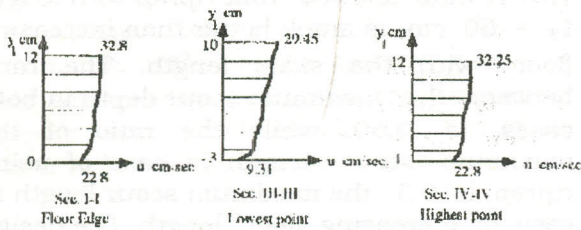


Figure 12 Velocity distribution curves over riprap

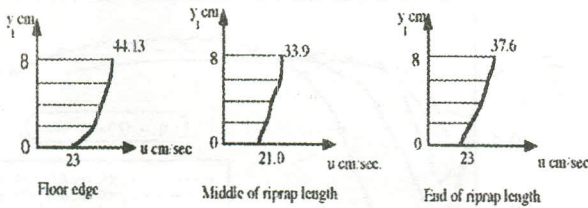


Figure 13 Velocity distribution curves over riprap

CONCLUSIONS

An expression is given for the relative maximum scour depth which is based on theoretical grounds and calibrated with the results of the experiments. Length of scour hole is obtained as a function of maximum scour depth. For scour hole development, the variation of maximum scour depth and length with the passage of time are presented. The velocity distribution in the scour hole pattern and over riprap length is well described. The installation of riprap protection is relatively much better in comparison with increasing floor with the same length. More investigation is needed in order to give accurate estimate for optimum riprap length and size as a protection work.

REFERENCES

- [1] A.J. Raudkivi, " Loose Boundary Hydraulics ", Pergamon Press, 1990
- [2] K. Suzuki, M. Michine and K. Kawazy, "Study on the Local Scour and Flow Downstream of Consolidation Work", Proceedings of the 26th Japanese Conference on Hydraulics, pp. 75-80, 1982. (in Japanese).
- [3] J. Farhoudi, " Local Scour Profiles Downstream of Hydraulic Jump ", J. of Hydraulic Research, Vol. 23, No. 4, pp. 343-358, 1985.
- [4] N. E. Bormann and Pierre Y. Julien, J. " Scour Downstream of Grade-Control Structures ", of Hydraulic Engineering, ASCE, Vol. 117, No. 5, pp. 579-594, 1991
- [5] C.E. Rice and Kem C. Kadavy, " Protection against Scour at SAF Stilling Basins", J. of Hydraulic Engineering, Vol. 119, No. 1, pp. 133-139, 1993.
- [6] J.C.M. Hoffmans and K.W. Pilarczyk, "Local Scour Downstream of Hydraulic Structures ", J. of Hydraulic Engineering, ASCE, Vol. 121, No. 4, pp. 326-340, 1995.
- [7] C. Schlichting, " Boundary Layer Theory", McGraw-Hill, 1968.
- [8] T. Tsubaki, and M. Hirano, " Flow Characteristics and Sediment Behaviors at Step-Downs", Technology Reports, Fac. Eng. Kyushu University, Vol. 43, No. 3, pp.288-293, 1970. (in Japanese).